Supporting Information

Surface Plasmon Resonance Modulation Toward Efficient Transparent Perovskite Light-Emitting Diodes

Zi-Yi Jin,[1,4] Qi Sun,[2] Wei He,[1] Shuang-Qiao Sun,[1] Guang-Li Li,[1] Yue-Min Xie[1,3,4*] and Man-Keung Fung[1,2,4*]

Z.-Y. Jin, Shuang-Qiao Sun, Guang-Li Li, Prof. Y.-M. Xie, Prof. M.-K. Fung
[1] Institute of Functional Nano & Soft Materials (FUNSOM), Jiangsu Key Laboratory for Carbon-Based Functional Materials & Devices, Soochow University, Suzhou, 215123, Jiangsu, PR China
E-mail: ymxie@suda.edu.cn; mkfung@suda.edu.cn

Qi Sun, Prof. Man-Keung Fung
[2] Macau Institute of Materials Science and Engineering (MIMSE), MUST-SUDA Joint Research Center for Advanced Functional Materials, Zhuhai MUST Science and Technology Research Institute, Macau University of Science and Technology, Taipa 999078, Macau, China

Prof. Yue-Min Xie
[3] Jiangsu Key Laboratory of Advanced Negative Carbon Technologies, Soochow University, Suzhou, 215123, Jiangsu, PR China

Zi-Yi Jin, Prof. Yue-Min Xie, Prof. Man-Keung Fung
[4] Institute of Organic Optoelectronics, Jiangsu Industrial Technology Research Institute (JITRI), 1198 Fenhu Dadao, Wujiang, Suzhou 215200, China

Methods

Materials

Phenethylammonium bromide (PEABr, >99%) and Guanidine Hydrobromide (GABr, 98%) were purchased from Greatcell Solar. Cesium bromide (CsBr, 99.999%) and lead bromide ($PbBr_2$, 99.999%) were purchased from Advanced Election Technology Co., Ltd. 1,4,7,10,13,16-Hexaoxacyclooctadecane (18-crown-6) (99%) and lithium bromide (LiBr, 99.999%) were purchased from Sigma-Aldrich. Dimethyl sulfoxide (DMSO, 99.9%) was purchased from Innochem. PVK, Chlorobenzene (99.8%) and Toluene (99%) were purchased from Acros. TFB was purchased from American Dye Source. TPBi and LiF were purchased from Luminescence Technology Corp.

Device fabrication:

First, the perovskite precursor solution was prepared by dissolving $PbBr_2$, CsBr, PEABr, GABr and LiBr at a specific molar ratio of 1:1:0.4:0.2:0.1 along with 18-crown-6 in DMSO at a concentration of 3.5 mg/ml. The concentration of the Pb^{2+} component in the precursor was 0.2 M. Then, the mixture was stirred over 12 hours at room temperature. The patterned ITO glass substrate was sequentially sonicated in acetone, deionized water and ethanol for 10 minutes. The ITO glass substrates were then dried in an oven at 100 °C for more than 2 hours. The ITO glass substrate was subsequently UV ozonated for 15 minutes and then transferred to a glove box with a N_2 atmosphere. The TFB solution (8 mg/ml in chlorobenzene) was spin-coated on ITO at 1500 rpm for 60 s followed by annealing at 120 °C for 20 min. The PVK layer (4 mg/ml in toluene) was then spin-coated onto the TFB layer at 4000 rpm for 45 s and annealed at 150 °C for 20 min. Subsequently, the perovskite precursor was spin-coated onto the PVK layer using a two-step process (1000 rpm for 5 s and 4000 rpm for 55 s) followed by annealing at 100 °C for 1 min. TPBi (50 nm), LiF (1.2 nm), Yb:Ag (7:3, 18 nm), and various thicknesses of CPL were fabricated through thermal

vacuum deposition under ultra-high vacuum conditions (below $4*10^{-6}$ mbar) to fabricate control PeLED devices. Finally, AgNP-based SPR layers with different deposition rates and MoO_3 (20 nm) were deposited onto CPL. The emission areas of the devices were 10 mm^2. After the fabrication of the devices, they were immediately encapsulated with a glass cover using a UV-curable epoxy adhesive inside a N_2-filled glovebox (<0.01 ppm O_2/H_2O).

Device characterization

EL spectra, current density-voltage characteristics, and CIE coordinates of the devices were measured with a Keithley 2400 source meter combined with a Photo Research PR655 spectrometer. Ultraviolet-visible (UV-vis) transmission and absorption spectra were recorded via a UV-Vis/NIR spectrophotometer (Perkin Elmer Lambda 950). Surface morphology images of the samples were obtained using an atomic force microscopy (AFM, Cypher-S). The half-lifetime of transparent perovskite light-emitting diodes (TPeLEDs) was measured using a commercial LED lifetime test system (64-channel ZJLS-4 tpye). Photoluminescence spectra and transient photoluminescence (TRPL) decay were measured with a steady/transient fluorescence spectroscopy system (FL-TCSPC, HORIB-FM-2015).

Optical simulation

The optical simulations were performed via the time domain finite difference method (Lumerical FDTD Solutions 8.7.3), and the optical parameters of the materials selected for the simulations were determined by an ellipsometer. To model the transmission of the cathode section accurately, a plane wave was employed as the light source and adjusted to match the emission wavelength. Perfect matching layer (PML) boundary conditions are used in both the X and Y planes. For the simulation of dispersion relation of the SPP, the

source was composed of 20 dipoles that are randomly distributed and oriented. For the simulation of the electric field intensity distribution of devices, a dipole positioned at the center of the emission layer served as the light source, with dipole orientations along the x, y, and z axes. Bloch boundary conditions were implemented on the sides perpendicular to the glass substrate, while PML boundary conditions were implemented on the remaining sides. A two-dimensional monitor was employed to observe the electric field intensity in the x-z plane perpendicular to the device. The far-field radiation pattern is determined by averaging the electric field over a 2 μm area at the parallel interface and in the direction of three dipoles.

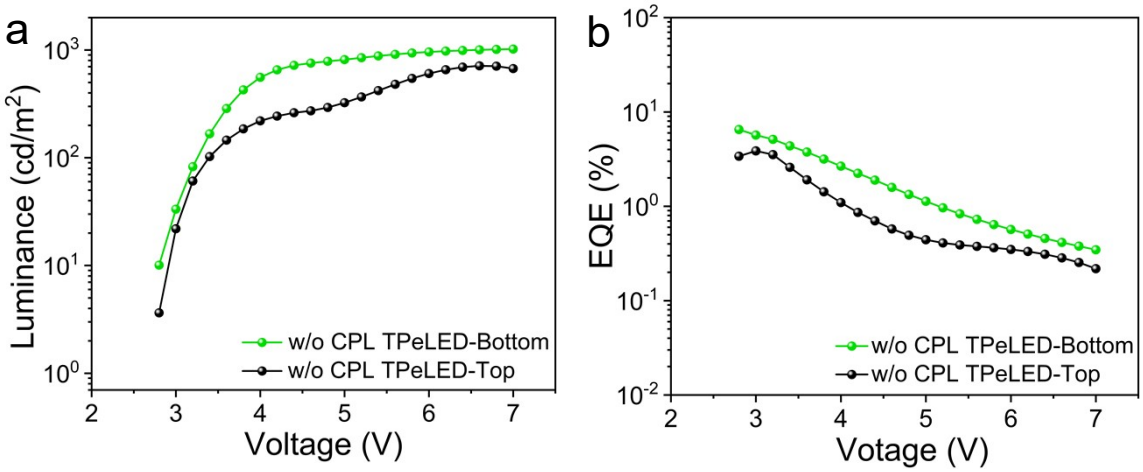

Fig. S1 (a) Luminance-voltage (*L-V*) curves, and (b) EQE-voltage (*EQE-V*) curves of transparent perovskite light-emitting diodes (TPeLEDs) without CPL.

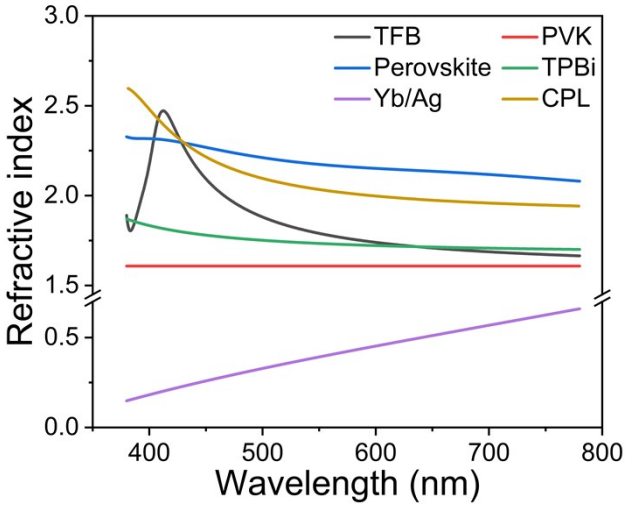

Fig. S2 Refractive indices of functional materials.

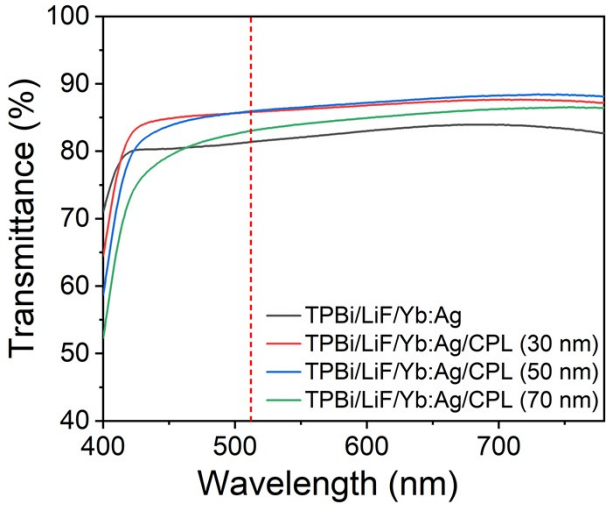

Fig. S3 Experimental optical transmission properties of the cathode sections (TPBi/LiF/Yb:Ag/CPL) as a function of CPL thickness. The thickness of TPBi is set to 50 nm.

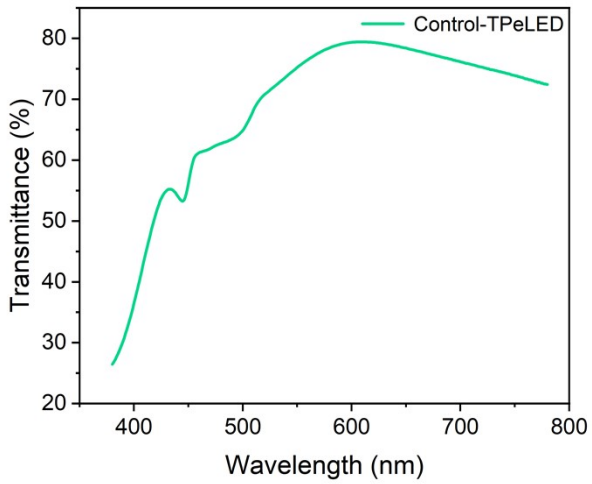

Fig. S4 Optical transmission spectra of 50 nm CPL incorporated TPeLED.

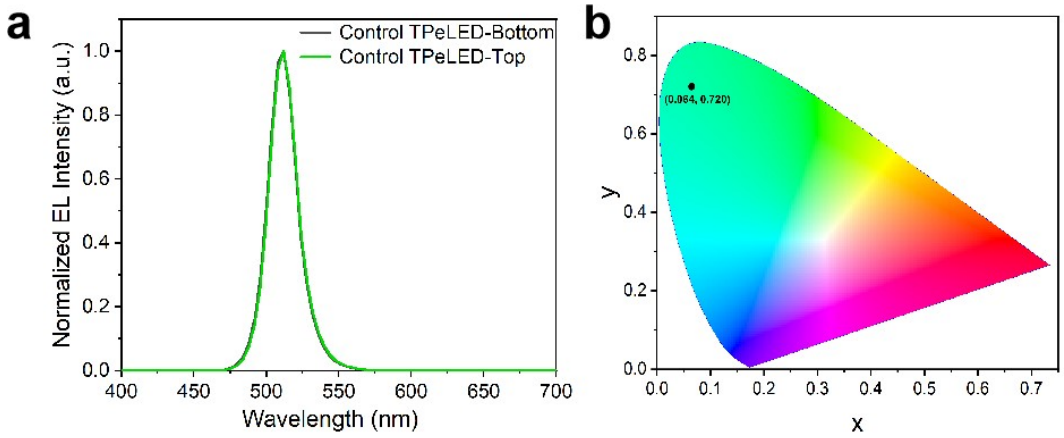

Fig. S5 (a) EL spectra measured from the top and bottom electrodes of the control TPeLED. (b) Commission International de l'Eclairage (CIE) coordinates for the control TPeLED.

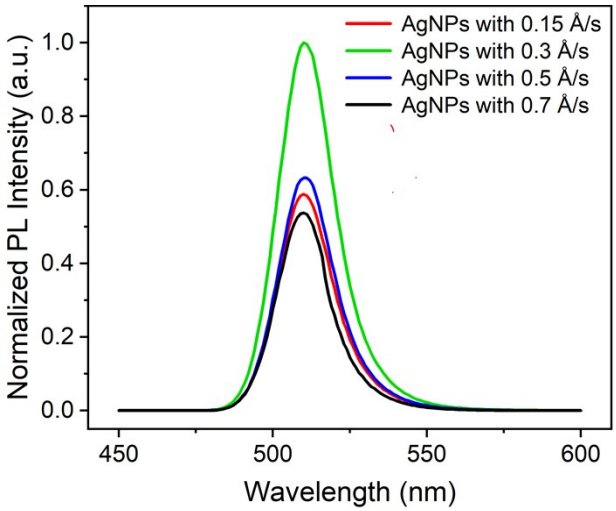

Fig. S6 Normalized photoluminescence (PL) spectra of perovskite film incorporated AgNP-based SPR layers at different deposition rates (0.15 Å/s, 0.3 Å/s, 0.5 Å/s, and 0.7 Å/s).

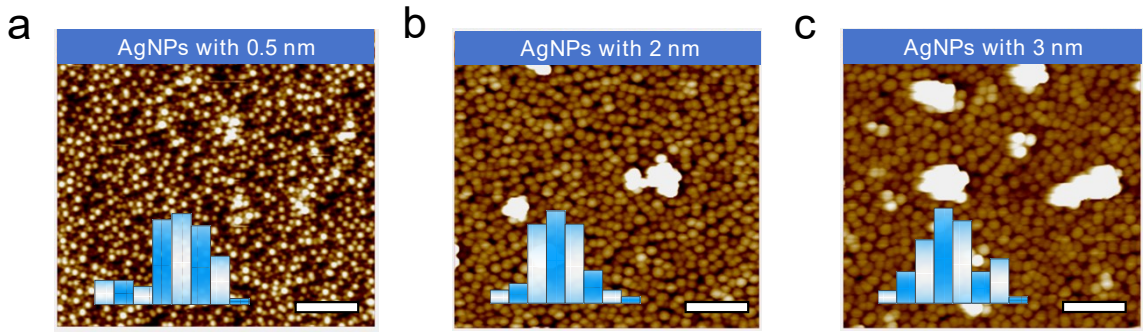

Fig. S7 AFM images and corresponding particle sizes of the AgNP-based SPR layers deposited at (a) 0.5 nm, (b) 2 nm and (c) 3 nm. The scale bar is 100 nm.

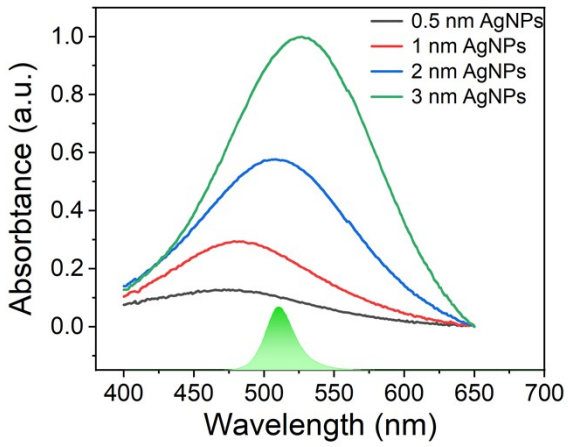

Fig. S8 Absorption spectra of AgNP-based SPR layers with different Ag thicknesses (0.5 nm, 1 nm, 2 nm, and 3 nm).

Table S1. Summary of fast (τ_1), medium (τ_2), slow (τ_3) and average (τ_{ave}) PL lifetime of the perovskite top sections without and with 1 nm thick AgNPs.

Samples	τ_1	A_1	τ_2	A_2	τ_3	A_3	τ_{ave}
w/o AgNPs	4.31	1752.83	16.03	666.21	94.75	78.04	35.3
w AgNPs	3.95	1714.48	13.93	574.62	75.25	78.56	28.2

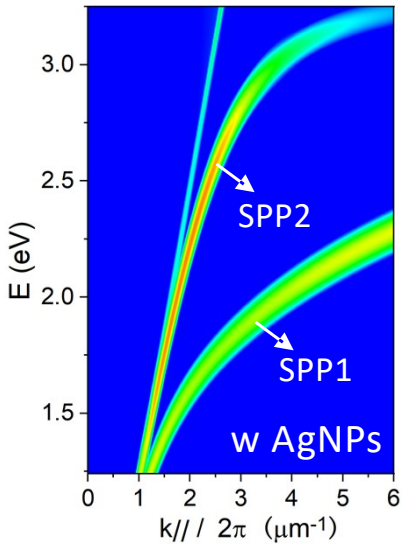

Fig. S9 Energy dispersion comparison of Yb:Ag/30 nm CPL system with AgNPs.

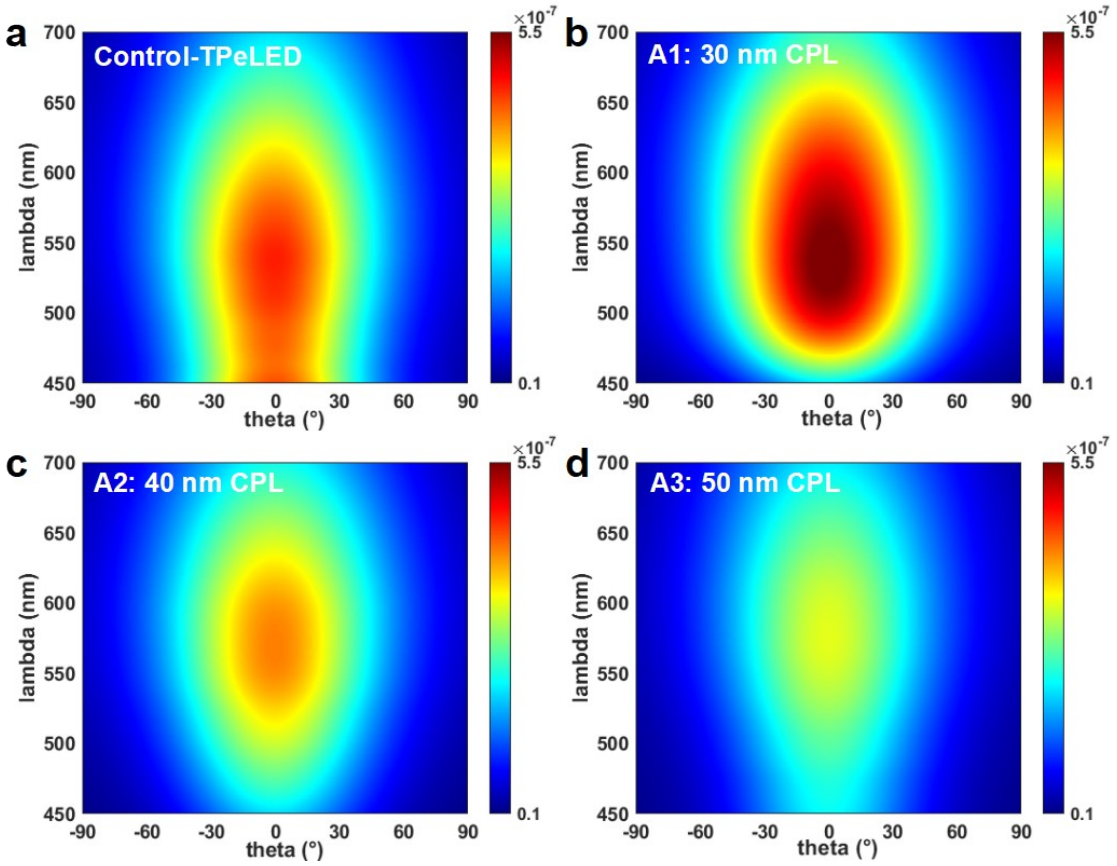

Fig. S10 Far-field electric field radiation at the top electrode for (a) control TPeLED, and (b) A1: 30 nm CPL, (c) A2: 40 nm CPL, and (d) A3: 50 nm CPL.

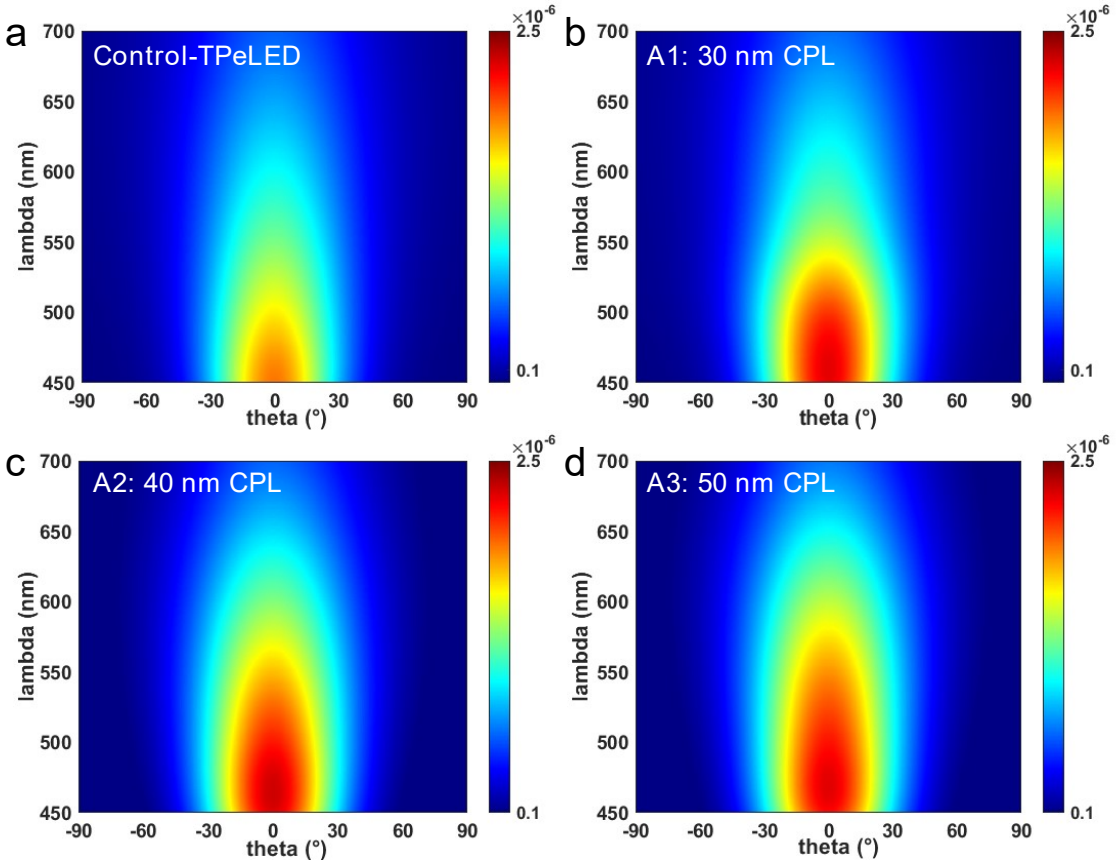

Fig. S11 Far-field electric field radiation comparison at the bottom electrode for (a) control TPeLED and (b) A1: 30 nm CPL, (c) A2: 40 nm CPL, and (d) A3:50 nm CPL.

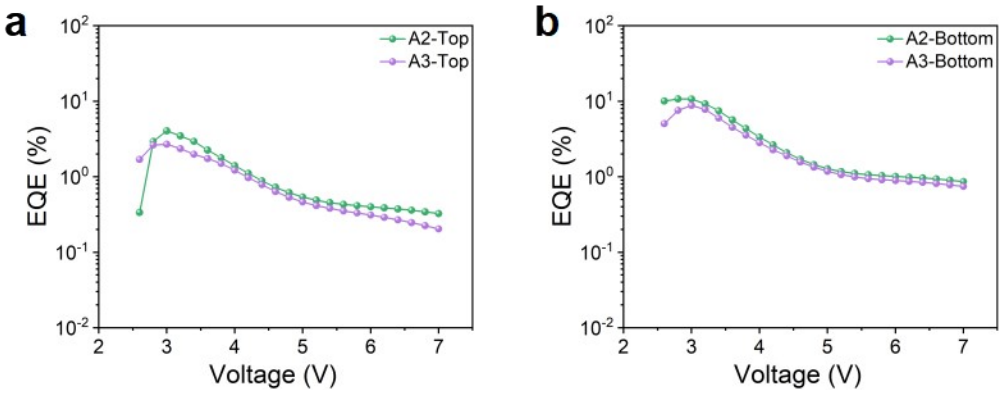

Fig. S12 *EQE-V* characteristics of A2 and A3 measured from (a) bottom and (b) top electrode sides.

Table S2. Device performance of AgNP-TPeLEDs with different CPL thicknesses.

Device	EQE_{bottom} (%)	EQE_{top} (%)	EQE_{total} (%)	V_{on} (V)
A1	11.1	7.5	18.6	2.8
A2	10.7	4.1	14.8	2.8
A3	8.8	2.7	11.5	2.8

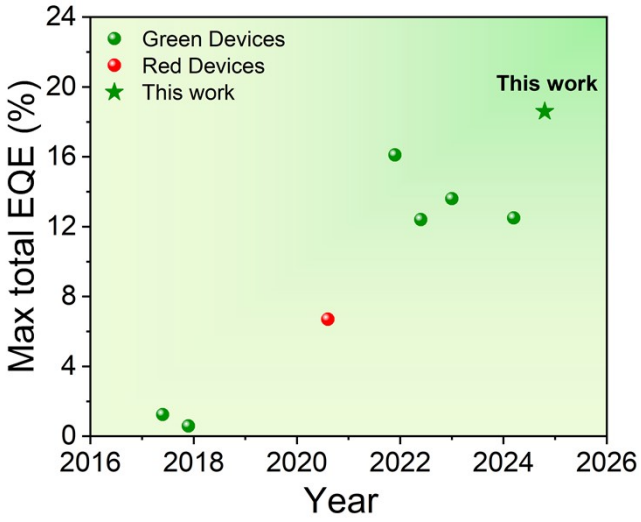

Fig. S13 Efficiency chart of reported TPeLEDs.

Table S3. Summary of the device performance of TPeLEDs.

EL peak	Device structure	Max. Top EQE	Max. Bottom EQE	Total EQE	Transmittance	T_{50}	Year[ref]
530 nm	ITO/PEDOT:PSS/$CH_3NH_3PbBr_3$/TPBi/LiF/Al/Ag/MoO_3	0.36%	0.85%	1.21%	47% (Average, 380-780 nm)	NA	2017[1]
518 nm	ITO/ZnO/PEI/$CsPbBr_3$ NCs/CBP/TCTA/MoOx/Au	0.23%	0.35%	0.58%	73% (Average, 380-780 nm)	NA	2017[2]
799 nm	ITO/AZO/PEIE/$FAPbI_3$/poly-TPD/MoO_3/Al/ITO/Ag/ITO	1.20%	4.50%	5.70%	55% (Average, 450-650 nm)	4 min	2020[3]
518 nm	ITO/PEDOT:PSS/PTAA/FA-doped $CsPbBr_3$ NCs/TPBi/Ca/Ag	2.80%	9.60%	12.40%	52% (Average, 400-780 nm)	8 min	2022[4]
512 nm	ITO/PVK/TFB/PVSK/TPBi/LiF/Mg:Ag/MoO_3	6.50%	9.60%	16.10%	＜50% (Average, 380-780 nm)	NA	2022[5]
516 nm	ITO/NiOx/Poly-TPD/PVK/PVSK/TPBi/LiF/Ca/Cu	5.70%	7.90%	13.60%	＞50% (Average, 380-780 nm)	NA	2023[6]
512 nm	ITO/PVK/PVSK/TPBi/LiF/Mg:Ag/TPBi/Mg:Ag	3.60%	8.90%	12.50%	＜50% (Average, 380-780 nm)	28 min	2024[7]
512 nm	**ITO/TFB/PVK/PVSK/TPBi/LiF/Yb:Ag/CPL/Ag/MoO_3**	**7.50%**	**11.10%**	**18.60%**	**66% (Average, 380-780 nm)**	**140 min**	**This work**

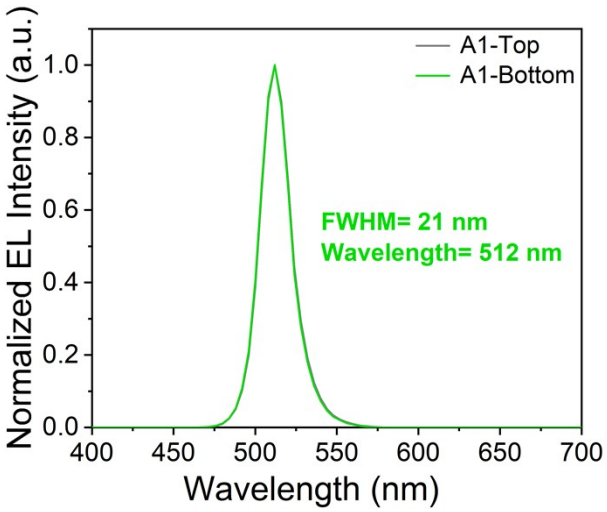

Fig. S14 EL spectra of A1 obtained from the top and bottom electrodes**.**

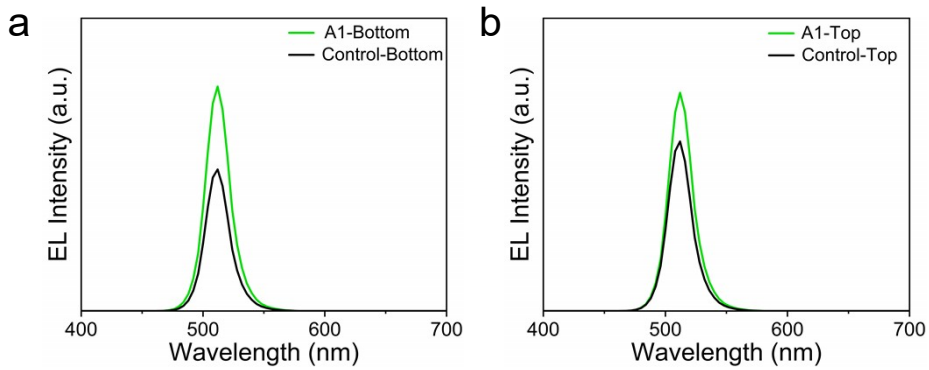

Fig. S15 EL spectra of A1 and control device measured from (a) bottom and (b) top electrode sides.

Reference

[1] J. Liang, X. Guo, L. Song, J. Lin, Y. Hu, N. Zhang, X. Liu, *Appl. Phys. Lett.* **2017**, *111,* 213301.

[2] H. Wu, Y. Zhang, X. Zhang, M. Lu, C. Sun, X. Bai, T. Zhang, G. Sun, W. W. Yu, *Adv. Optical Mater.* **2018**, *4*, 1700285.

[3] C. Xie, X. Zhao, E. W. Y. Ong, Z.-K. Tan, *Nat. Commun.* **2020**, *11*, 4213.

[4] Q. Wan, L. Huang, L. Kong, Q. Zhang, C. Zhang, M. Liu, X. Liao, W. Zhan, W. Zheng, C. Yuan, M. He, L. Li, *ACS Appl. Mater. & Inter.* **2022**, *14*, 19697.

[5] L. Cai, J. Zhou, G. Bai, J. Zang, A. El-Shaer, T. Song, M.-K. Fung, B. Sun, *Adv. Optical Mater.* **2022**, *10*, 2101137.

[6] H. Wang, W. Xu, Q. Wei, S. Peng, Y. Shang, X. Jiang, D. Yu, K. Wang, R. Pu, C. Zhao, Z. Zang, H. Li, Y. Zhang, T. Pan, Z. Peng, X. Shen, S. Ling, W. Liu, F. Gao, Z. Ning, *Light: Sci. Appl.* **2023**, *12*, 62.

[7] Y. Qi, R. Liu, Z. Li, Y. Song, C.-k. Wang, L. Cai, *Opt. Laser. Technol.* **2024**, *169*, 110002.